

## Structural Design of a Tender Lift for Medium- And Large-Sized Yachts

S. Baragetti<sup>1,2</sup>

<sup>1</sup>Department of Engineering, University of Bergamo, Viale Marconi 5, 24044, Dalmine (BG), Italy.

<sup>2</sup>GITT – Centre on Innovation Management and Technology Transfer of the University of Bergamo, Via Salvecchio 19, 24129 Bergamo, Italy.

### Abstract

Tender lifts are yacht accessories that are mainly used to drop small boats and persons into the water. The extensive personalisation of yachts can lead to some critical issues for the design of tender lifts, which must be specifically made according to the unique geometry of each yacht. The aim of this work was to analyse and optimise the structure of a prototype tender lift for medium-sized yachts, as realised by Besenzoni S.p.A (Sarnico, BG) with AISI 304. The optimisation process involved analytical and numerical models, which were verified by experimental measurements. In particular, the stress and strain states of the actuation device were evaluated along the entire range of motion of the mechanism. The results were used to modify the geometry of the prototype. The optimised prototype demonstrated reduced applied stresses and increased values for the safety factor along the entire mechanism.

**Keywords:** nautical sector; tender lift; numerical models; analytical models; experimental measurements; optimisation

### I. Introduction

The installation of a tender lift on the stern is a very common feature of medium- and large-class yachts. This mechanical system fulfils two main tasks: it eases the boarding and the descent of bathers into the open sea, and it is also used to lower small crafts into the water (Figs. 1 and 2).



Fig. 1: Picture of a yacht with a tender lift mounted on the stern.

The various tender lift models that are commercially available present a great diversity in their main characteristics. The basic concept behind the tender lift is simple, with the planking level being moved via the operation of two parallel four-bar linkage devices. However, the extensive personalisation of yachts can lead to some critical issues for the design of tender lifts, which must be specifically adapted to the unique geometry of each boat.

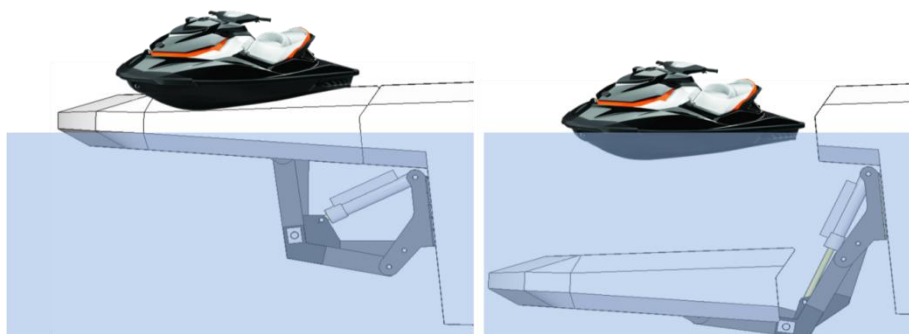


Fig. 2: Operation of the tender lift.

The aim of this work was to analyse and optimise a new prototype structure for tender lifts, as realised by Besenzoni S.p.A (Sarnico, BG). AISI 304 plates and welded section beams were used for the realisation of the prototype. Analysis was performed through three different approaches, in which the movement mechanism of the tender lift was carefully examined (ISO 2010; RINA 2010; API 2000; Baragetti, Medolago 2012). Classical mechanics analytical methods were initially applied, followed by the development of detailed finite element method (FEM) models of the mechanical system. To validate the implemented models, experimental tests were conducted on the prototype.

The results obtained from the first prototype provided a complete overview of the stress and strain states of the system, which allowed the identification of the major critical aspects. An optimisation process was implemented, beginning with a sensitivity analysis, to identify the critical structural parameters of the tender lift. A calculation code was used to design a new optimised lift with enhanced structural performance. Care was taken in analysing the influence of the stiffness of the planking level on the stress state of the elements of the movement mechanism.

## II. Prototype description

The prototype hydraulic tender lift is constituted of three main elements: two parallel four-bar linkage devices and a planking level

level (Fig. 3a). The movement mechanism of the planking level for this prototype is presented in

Fig. 3b. A hydraulic actuator drives the four-bar linkage system, whose constrained nodes are mounted on the hull of the craft, while the upper beam is built-in with the planking level. The tender lift is designed to be mounted in the boat's

stern, to lower small crafts or people, for a maximum capacity of 850 kg. The prototype was realised in AISI 304 steel (Table 1), and the beam sections for the device were hollow and rectangular.

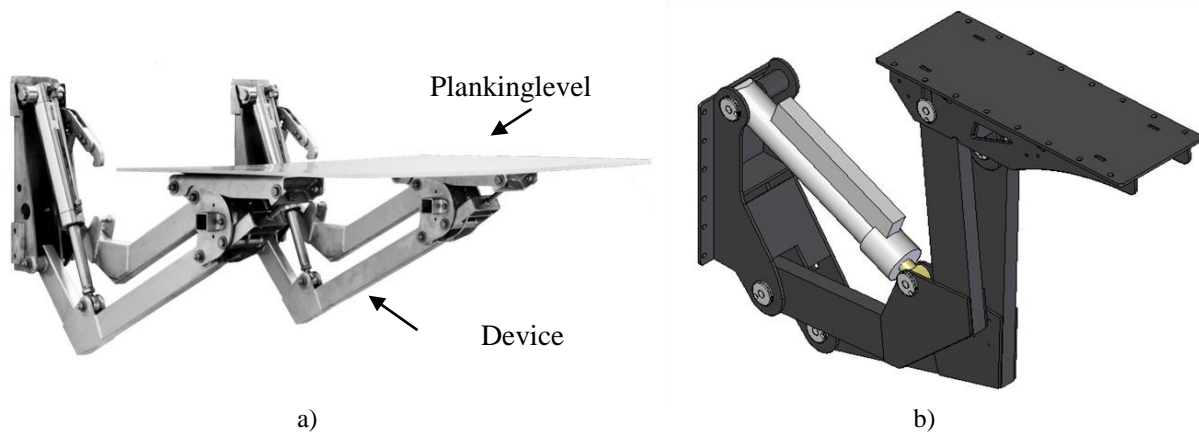


Fig. 3: Example of devices for: (a) the movement of the planking level of a tender lift, and (b) the mechanism of the tender lift prototype studied in the present work.

Table 1 Mechanical characteristics of AISI 304 steel  
 (source: www.matweb.com)

Yield tensile strength	$R_{p0.2}$	215	[MPa]
% Elongation at break	A%	45%	
Young's modulus	E	206000	[MPa]

## III. Prototype analysis

### 3.1 Theoretical and numerical models

To study the critical points of the prototype, a calculation code was developed. This code allowed the stress state in critical sections of the mechanism to be determined at discrete positions along the device (Fig. 4). By using this tool, a graph of the safety factor in each of the critical sections was created (Fig. 5). The safety factor was less than 1.5 in every operating position of the device.

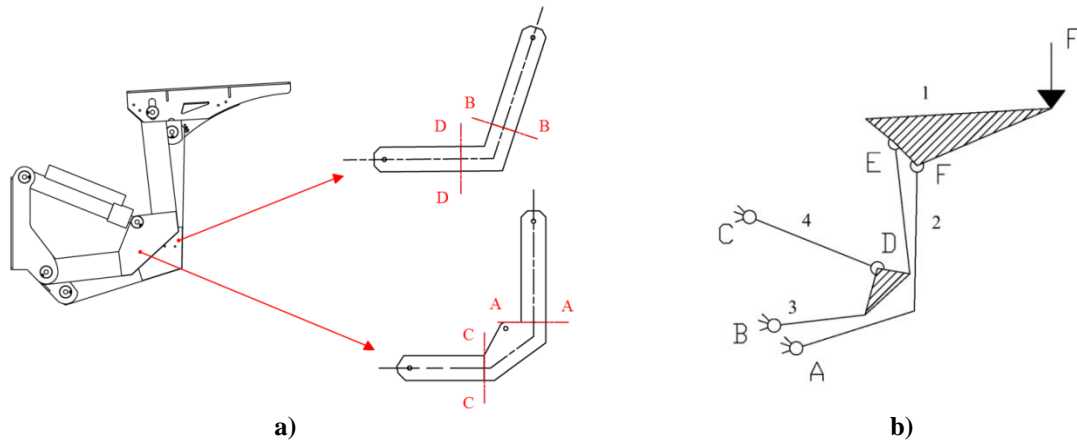


Fig. 4: (a) Critical sections of the device arms and (b) model adopted for the calculation code.

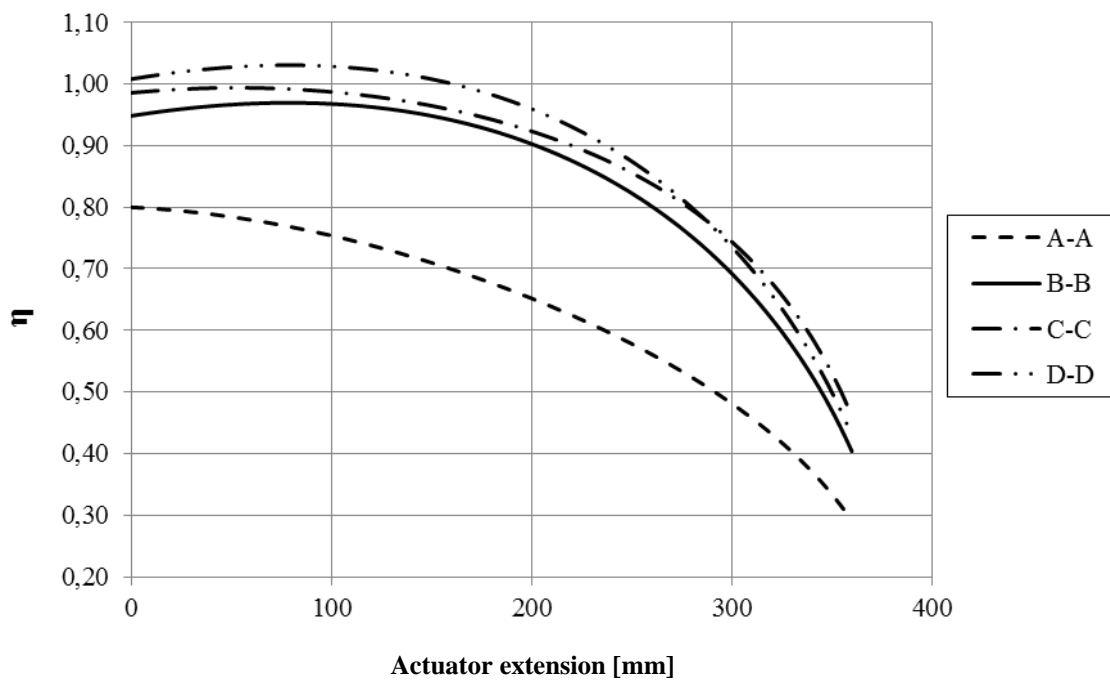


Fig.5: Safety factors  $n$  in the critical sections of the mechanism, along the whole device.

To investigate the stress state of the four-bar linkage system more pragmatically, a shell numerical FEM of the movement device was developed. In this step, the following simplified hypotheses were adopted: (1) the material was assumed to show a linear elastic behaviour (Table 1), (2) a single device was modelled (i.e., the presence of the planking level was ignored), (3) a load of 2/3 of the nominal load was assumed, and (4) only two positions of the

actuator were simulated (zero actuator travel and fully extended actuator). The load was applied at the tip of the shoe (i.e., the connecting rod of the four-bar linkage), as shown in Fig. 4b. The base plate of the device was constrained to the ground with a fixed restraint. Sharp edges in the prototype were reproduced in the numerical model. The results of the mechanism simulations (Fig. 6) revealed that the yield value of the material was exceeded in several regions for both simulated configurations.

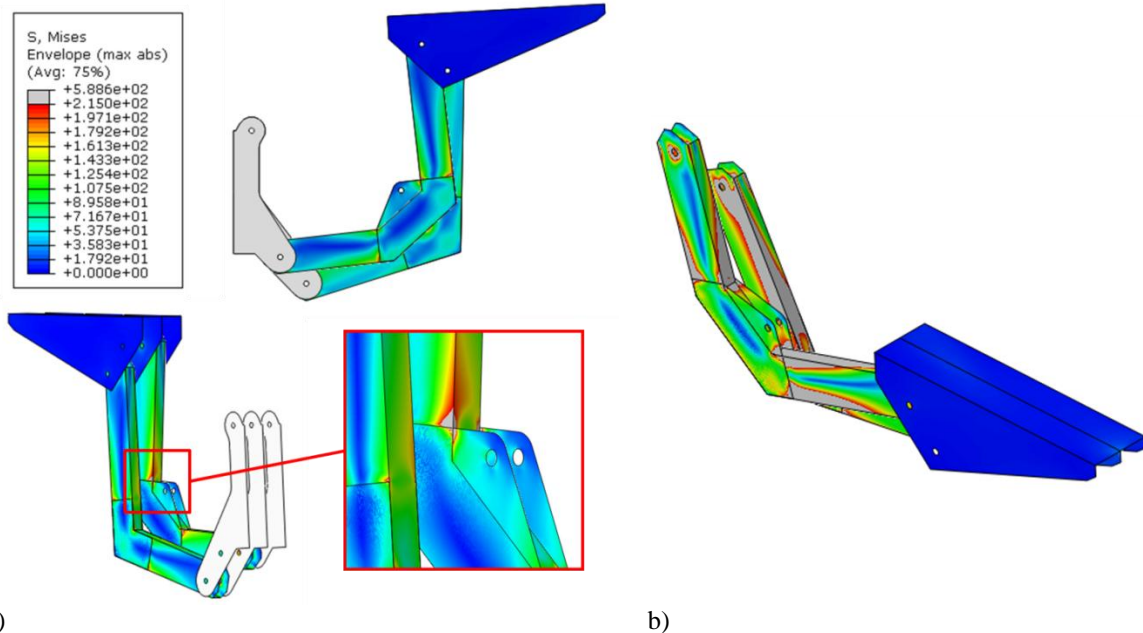


Fig. 6: FEM model results of the tender lift movement device, in terms of equivalent von Mises stress [MPa], considering the two simulated configurations: (a) zero actuator travel and (b) fully extended actuator.

### 3.2 Strain gauge measurements

Experimental measurements were performed on the prototype to validate the FEM simulation results (Fig. 7). LY11-3/120 HBM linear strain gauges (<http://www.hbm.com/it/>) were used to measure the deformations. These strain gauges were placed at specific points of the device (Figs. 8 and 9), and the stress state was calculated by assuming a linear elastic/perfectly plastic material behaviour. The orientation of the strain gauges was chosen such that the strain gauge measurement grid was aligned

with the dotted lines on the device arms (Figs. 8 and 9). Figure 10 compares the strain gauge measurements and the numerical results for the strain gauge mounted in the most-loaded region (strain gauge 2). In this figure, the vertical dotted line identifies the design load of a single tender lift device (i.e., 2/3 of the maximum nominal carrying capacity). Points of the FEM curve related to load values that differed from the values applied in the simulation were obtained through the linear interpolation of the results, with the model assumed to be linear elastic.



Fig.7: Tender lift mechanism prototype, with applied strain gauges for the experimental measurements.

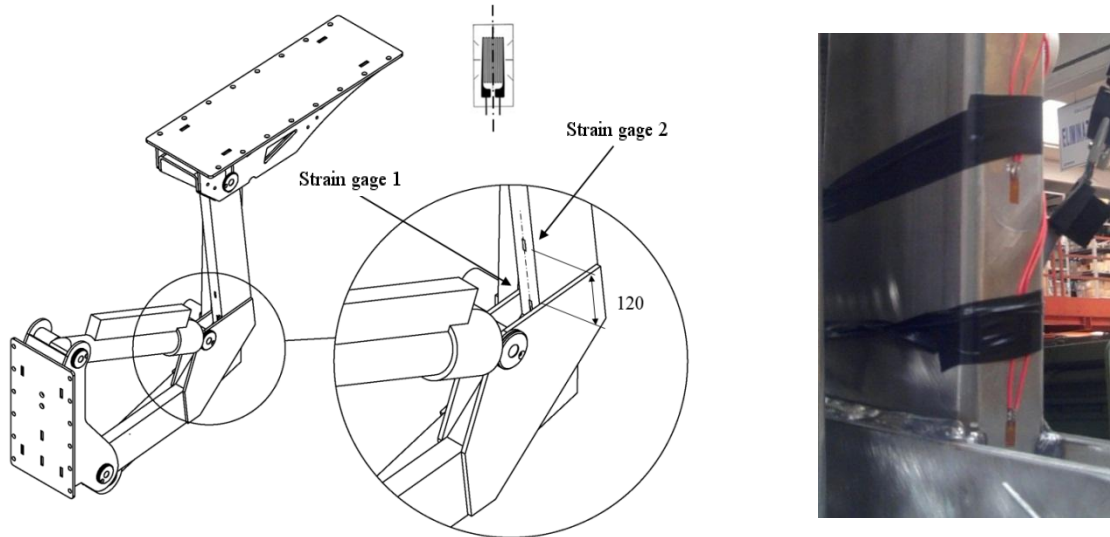


Fig.8: Placement of strain gauges 1 and 2 on the prototype.

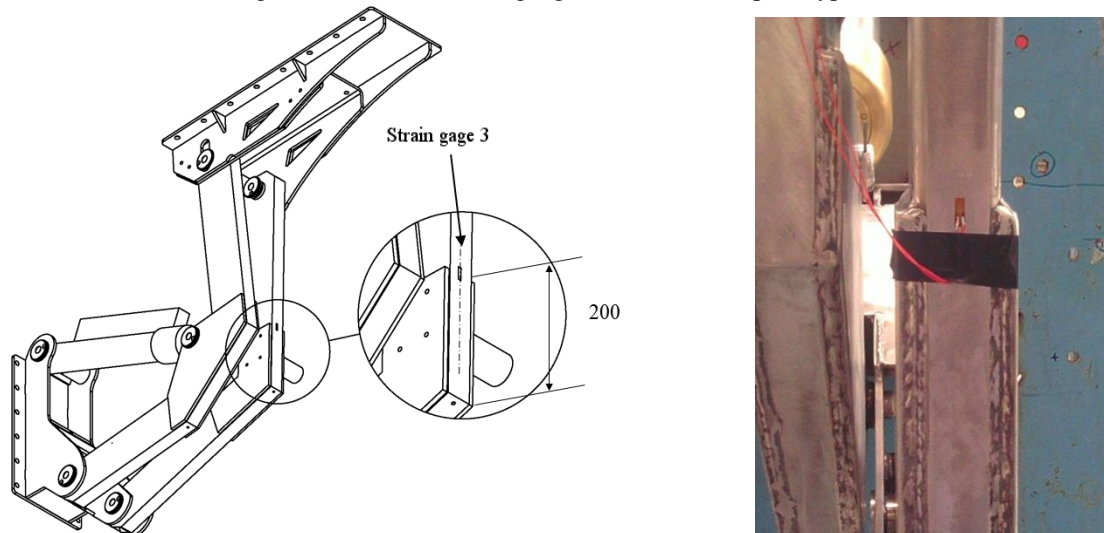
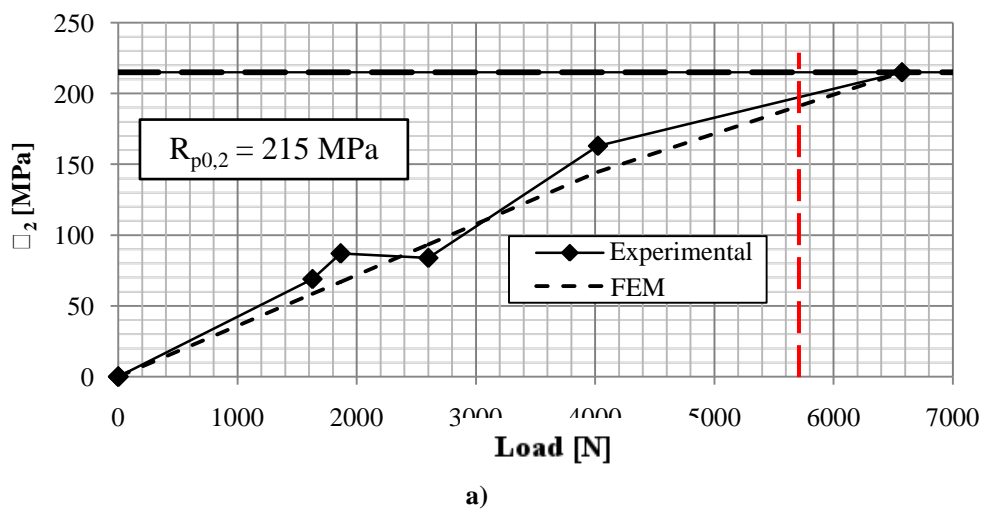
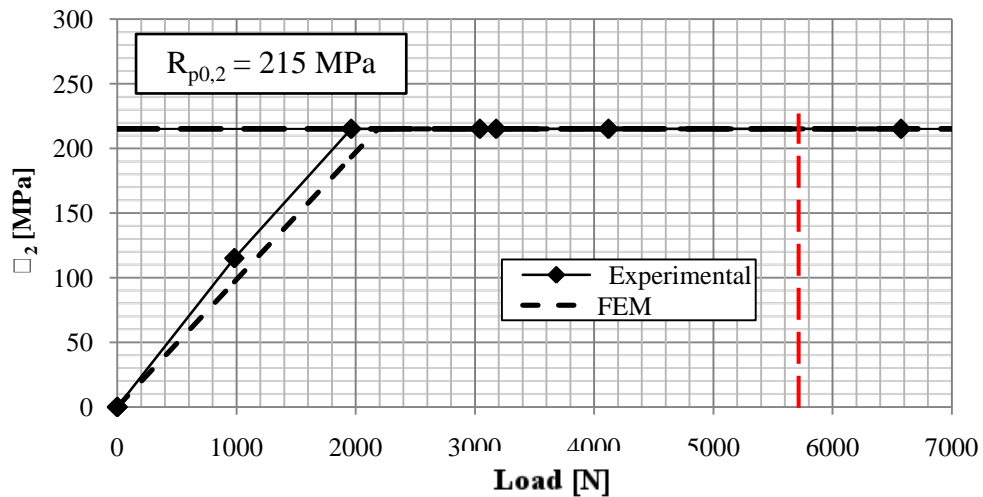


Fig.9: Placement of strain gauge 3 on the prototype





b)

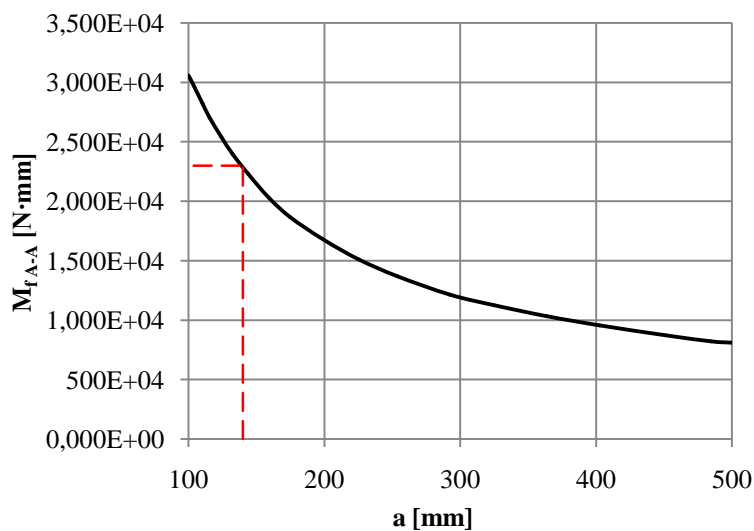
Fig. 10: Strain gauge measurement ( $\sigma$ ) vs. applied load for strain gauge 2, relative to the (a) fully raised or (b) fully lowered tender lift.

The data collected from strain gauge 2 suggested that the FEM model was coherent with the real stress state, and that the section where the strain gauge was mounted worked beyond the yielding limit of the material.

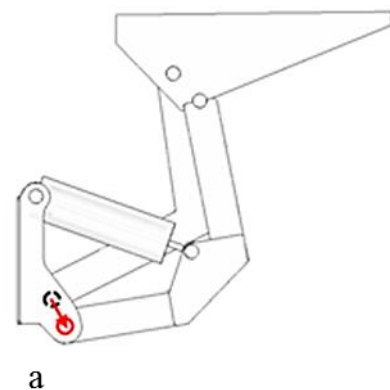
#### IV. Optimisation

The validated calculation code was used to perform a sensitivity analysis. The purpose of this sensitivity analysis was to identify the main geometrical parameters that influenced the stress

state in the critical sections. The value of each identified parameter was plotted on the x-axis against the value of the bending moment in the critical A-A section on the y-axis (Fig. 4a). Examples of these graphs are shown in Fig. 11 for only two variables. This analysis revealed that the prototype geometry was far from optimal, and that the stress values at the critical points could be decreased by employing suitable modifications.



a)



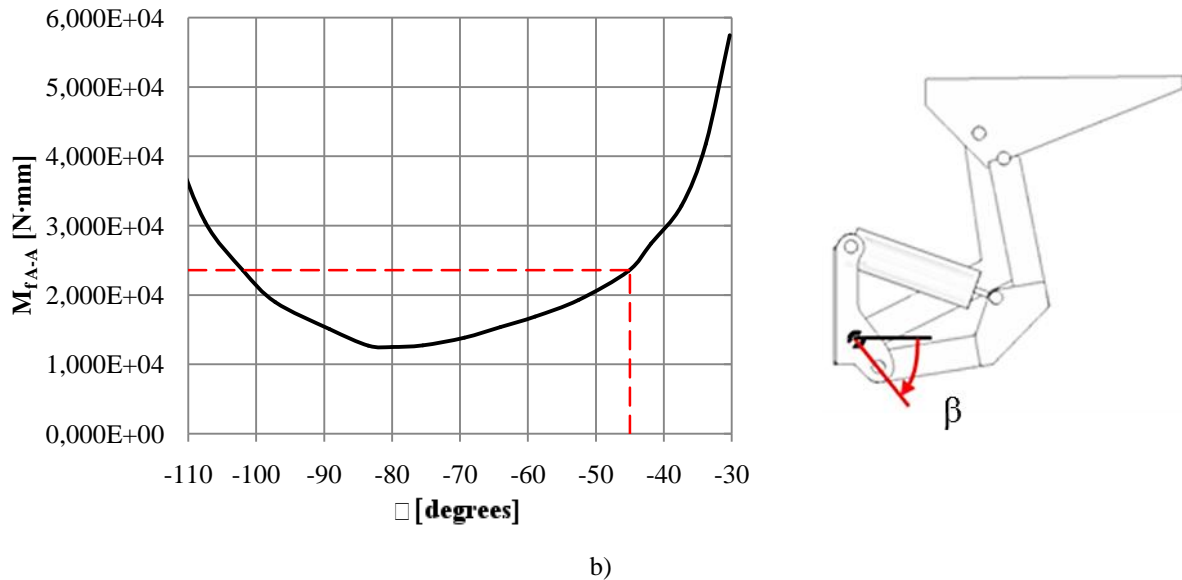


Fig. 11: Sensitivity analysis. Value of the bending moment  $M_{FA-A}$  in the critical section A-A (Fig. 4a), as a function of the examined parameter, (a)  $\alpha$  or (b)  $\beta$ . The prototype state is specified by the red line.

### V. Planking level effect

After the geometry had been optimised, the influence of the planking level on the stress state of the device arms was analysed. Unfortunately, neither the geometry nor the material of the planking level was known beforehand, because the ship owner will determine how the system will be mounted. Therefore, a reference geometry was proposed, and

the effect of variations in the stiffness on the stress state of the device was analysed. The results of numerical models (Fig. 12) indicated that the stress state of the tender lift increased with decreasing stiffness of the planking level. The stiffness range considered during the investigation produced a maximum increase in the Mises equivalent stress of 40% in the critical regions.

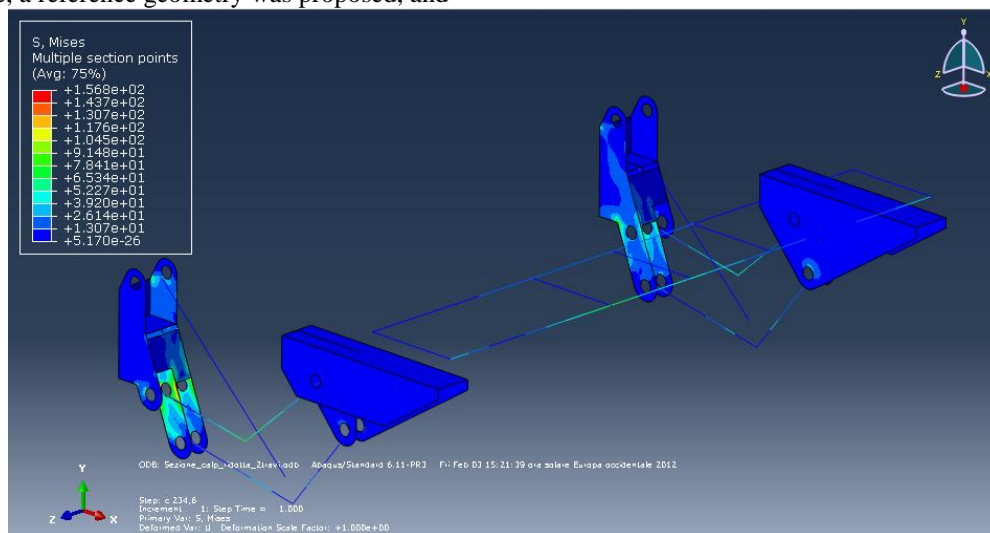


Fig. 12: Numerical model of the tender lift with the planking level (stresses in [MPa]).

### VI. Optimised prototype

The investigation allowed the critical points of the tender lift prototype to be defined and the parameters governing its strength to be identified. By using the analysis results, a new optimised geometry was proposed (Fig. 13a), which employed the following modifications (Fig. 13b) compared to the original prototype: (1) the hydraulic actuator was

linked at the inferior beam, (2) the  $\beta$  angle was chosen so as to maintain its value as close to  $90^\circ$  as possible during its range of motion, (3) the beam b (and also beam d, because  $b = d$ ) was extended, and (4) the sharp edge of the rocker arm without actuation was rounded.

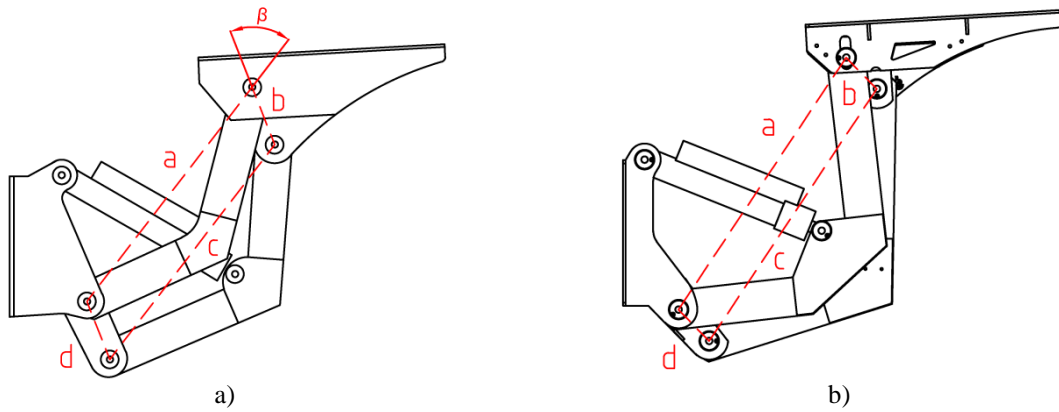


Fig. 13: (a) Optimised geometry for the tender lift device compared to (b) the original prototype geometry.

Although these modifications involved a negligible variation of the system mass and dimensions, they allowed the mechanism to achieve a marked increase in structural strength. In particular,

safety factors of greater than 1.2 were achieved in all of the critical sections of the modified prototype (Fig. 14).

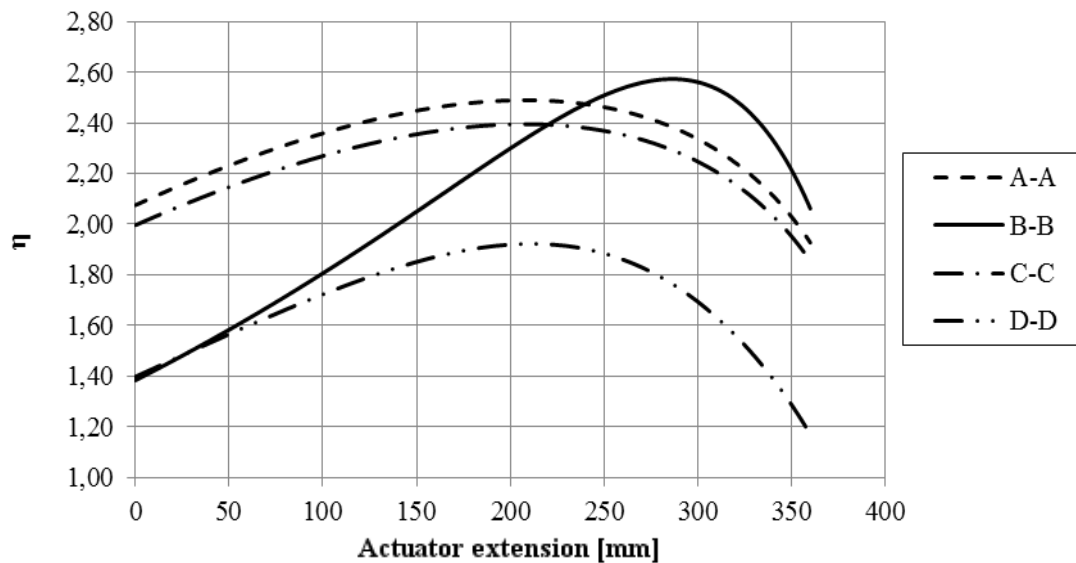


Fig. 14: Safety factors for the optimised prototype along the range of motion for sections A-A, B-B, C-C, and D-D. These sections are shown in Figs. 4a and 15 for the original and optimised prototypes, respectively.

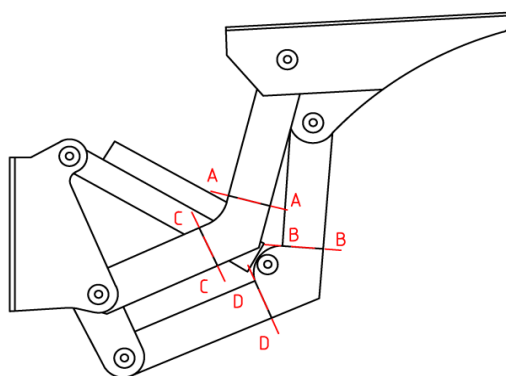


Fig. 15: Critical sections of the arms of the optimised prototype mechanism.

## VII. Conclusions

This work presented the optimisation process for a prototype tender lift that was designed for installation on medium-large size yachts. The examined structure can be used for different purposes; for example, it may be used as a moving level to lower small crafts or people into the water. The stress and strain states of the actuation device were carefully evaluated along the range of motion. Analytical and numerical methods, together with experimental measurements, were used to modify the geometry of the prototype. The new prototype demonstrated reduced applied stresses and increased values for the safety factor, which were greater than 1.2.

## References

- [1] ISO 19901-3 (2010), *Petroleum and Natural Gas Industries - Specific Requirements for Offshore Structures - Part 3: Topsides Structure*.
- [2] RINA (2010), *Rules for the Classification of Ships, Part B*.
- [3] API RP 2A-WSD (2000), *Recommended Practice for Planning, Designing and Constructing Fixed Offshore Platforms-Working Stress Design*.
- [4] Baragetti, S., Medolago, A., "Progettazione di una plancetta/tender lift per yacht di dimensioni medio-grandi", 41° Convegno Nazionale AIAS, 5-8 settembre 2012, Padova.
- [5] HBM, *Strain Gauges and Accessories Manual*. Retrieved from <http://www.hbm.com/it/>.